Heterogeneous kinetics of the loop formation of a single polymer chain in crowded and disordered media

Seulki Kwon and Bong June Sung

Department of Chemistry, Sogang University, Seoul 04107, Republic of Korea

The cytoplasmic volume of cells is occupied and crowded by a variety of macromolecules, such as proteins and cytoskeleton structures. Such diverse macromolecules make the cell cytoplasm not only structurally heterogeneous but also dynamically heterogeneous: Some macromolecules may diffuse freely inside cell cytoplasm at certain timescales while others hardly diffuse. Studies on the effects of the dynamic heterogeneity on reaction kinetics have been limited even though the effects of the crowdedness and structural heterogeneity were investigated extensively. In this study, we employ a simple model of mixtures of mobile and immobile matrix particles, tune the degree of dynamic heterogeneity by changing the fraction of immobile matrix particles, and investigate reaction kinetics in such heterogeneous media. We employ the loop formation of a single polymer chain as a model reaction and perform Langevin dynamics simulations. We find that the free-energy barrier of the loop formation is decreased as the systems become more crowded with matrix particles. But the free-energy barrier is not sensitive to the dynamic heterogeneity. As dynamic heterogeneity increases with an increase in the fraction of immobile matrix particles, however, the diffusivity of the system decreases significantly. The decrease in the diffusion (due to the dynamic heterogeneity) and the decrease in the free-energy barrier (due to the crowdedness) lead together to a complicated trend of the loop formation kinetics. As the volume fraction of immobile matrix particles reaches a critical value at the percolation transition, the reaction kinetics becomes significantly heterogeneous and the survival probability distribution of the chain loop formation becomes stretched-exponential. We also illustrate that the heterogeneous reaction rate near the percolation transition relates closely to the structures of local pores in which the polymer is located.

I. INTRODUCTION

Cell cytoplasm and cell membranes consist of various components, of which size and interaction vary tremendously. In the case of cell cytoplasm, for example, up to 40% of its volume is filled with proteins, organelles, and cytoskeleton networks [1,2], which makes the structure inside cells intrinsically heterogeneous. Such a structural and compositional heterogeneity entails dynamic heterogeneity, i.e., the diffusion of certain macromolecules significantly differs depending on the size and the interaction of neighboring components. Both static and dynamic heterogeneity would affect the transport and the chemical kinetics of proteins in cells. However, the effect of the dynamic heterogeneity remains elusive, while the effect of crowdedness and static heterogeneity on the kinetics has been investigated extensively. In this study, therefore, we would like to investigate the effect of the static and dynamic heterogeneity on the reaction kinetics of a model reaction by performing molecular simulations. We show that as the dynamic heterogeneity becomes significant, the heterogeneous kinetics appears where a single reaction rate constant may not describe the reaction kinetics.

The shape and functions of proteins in crowded and heterogeneous environments are different from those in dilute solutions [3,4]. Previous experiments [1,5–7] and theoretical studies [8–10] showed that the crowdedness affected cell metabolism [11], transport phenomena [12,13], and cell signaling [14]. Previous studies [15–17] also showed that

the crowdedness of cell cytoplasm might bring about two competing effects on the kinetics: (1) the protein diffusion slows down as the system becomes more crowded, which should inhibit the diffusion-controlled reaction, but (2) the crowdedness may increase the effective collision between two reactants such that the reaction rate may be enhanced. In this study, we also observe such competing effects of crowdedness on the kinetics in our simulations, but find that the dynamic heterogeneity complicates the competing effects significantly. This suggests that the dynamic heterogeneity needs to be taken into account when one tries to investigate the kinetics in complex systems.

Systems with matrix particles that do not diffuse at all have been studied extensively [18–21]. Those matrix particles are fixed in space at random positions and become obstacles to fluid particles, thus constructing random (porous) media [22–29]. The transport of fluid particles in random media is described well by a percolation theory. When the volume fraction (ϕ) of the quenched matrix particles is below its critical value (ϕ_c, the percolation threshold volume fraction), a percolating network of free volume exists, through which a fluid particle diffuses. When $\phi > \phi_c$, the percolating network disappears and the long time diffusion of the fluid particles should vanish [30–33]. When $\phi = \phi_c$, the percolating free volume is fractal such that the diffusion of fluid particles become subdiffusive at all timescales. The value of ϕ_c depends on the relative size and the interaction potential of the fluid particle. However, studies on the kinetics in random media

have been relatively limited. In this study, we introduce a simple system of mixtures of quenched and free matrix particles. Free matrix particles diffuse at a reaction timescale while quenched matrix particles do not diffuse at all. The diffusion of matrix particles that occupy the system is, then, heterogeneous. We tune the degree of dynamic heterogeneity and investigate its effect on the kinetics by changing the fraction (γ) of the quenched particles.

We employ the loop formation of a single polymer chain as a model system in this study. The loop forms when two ends of the linear chain meet each other, which should involves a large conformational change. The loop formation is an intramolecular reaction of a single chain relevant to biopolymer reactions such as protein folding or DNA hairpin formation. Because reactive sites, two ends of a polymer, need to encounter each other to initiate the reaction, the end-to-end distance (r_{ete}) of the polymer chain, therefore, can serve as a reaction coordinate. And many theories have been developed to discuss the loop formation kinetics based on Smoluchowski-type diffusion equation[34–37] with a single diffusion coefficient (D_{ete}) and the equilibrium distribution function of r_{ete}. But when the kinetics becomes significantly heterogeneous as in our study, such theoretical description fails to describe the reaction kinetics of the loop formation properly. We also investigate the reverse reaction of the loop formation, i.e., unlooping reaction, which is hardly affected by surrounding matrix particles.

The rest of the paper is organized as follows. In Sec. II we discuss the simulation model and methods in details. Simulation results are presented and discussed in Sec. III. Section IV contains the summary and conclusions.

II. MODEL AND METHOD

Our simulation system consists of a single flexible polymer chain and matrix particles. There are two types of matrix particles: (a) mobile particles that can diffuse freely and (b) immobile particles that are fixed as obstacles in space. The polymer chain is modeled as a bead-spring chain comprised of 32 monomers of diameter σ and mass m, which are the units of length and mass in this study, respectively. The bonding interaction [$U_b(r)$] between chemically bonded monomers is described by a harmonic potential, i.e., $U_b(r) = K(r - r_0)^2$, where r is the distance between two monomers and $r_0 = \sigma$. We set $K = 1000 k_B T/\sigma^2$, where k_B and T denote the Boltzmann constant and temperature, respectively. Matrix particles are modeled as spherical particles of diameter σ_c and mass m. The value of σ_c is either σ and 4σ in this study. Note that matrix particles of $\sigma_c = \sigma$ are comparable in size with monomers while matrix particles of $\sigma_c = 4\sigma$ is slightly larger than the radius of gyration of the polymer chain, i.e., $R_{g,\text{bulk}} = 3.7 \pm 0.6$, when there is no matrix particle around the chain.

The non-bonding interactions between particles in our simulations are described by a truncated and shifted Lennard-Jones potential as follows:

$$U_{LJ}(r_{ij}) = \begin{cases} 4\epsilon\left[\left(\frac{\sigma_{ij}}{r_{ij}}\right)^{12} - \left(\frac{\sigma_{ij}}{r_{ij}}\right)^6\right] - \epsilon_{r_c}, & r < r_c, \\ 0, & r \geqslant r_c, \end{cases}$$

where r_{ij} is the distance between the ith and the jth particles, and $\epsilon_{r_c} = 4\epsilon\left[\left(\frac{\sigma_{ij}}{r_c}\right)^{12} - \left(\frac{\sigma_{ij}}{r_c}\right)^6\right]$. The interaction strength ϵ is

set to $k_B T$ and is the unit of energy in this study. σ_{ij} is the arithmetic mean of the diameters of i and j particles; i.e., $\sigma_{ij} = \frac{\sigma_i + \sigma_j}{2}$. We set $r_c = 2^{1/6}\sigma_{ij}$ such that the interactions between particles are purely repulsive except the interaction between two end monomers of the polymer chain. Only for the pair of end monomers of the chain, we set $\epsilon = 4k_B T$ and $r_c = 2.5\sigma$ such that the looped state of the polymer chain becomes energetically stable to some extent.

We perform Langevin dynamics (LD) simulations under the canonical ensemble via LAMMPS simulator as follows:

$$m\frac{d^2\mathbf{r}}{dt^2} = -\nabla_r U - \xi\frac{d\mathbf{r}}{dt} + \delta F_r(t), \tag{1}$$

where U is the total sum of inter-particle interactions including both bonding and non-bonding interactions. ξ is a friction coefficient and is set to $\xi = 2$. $\delta F_r(t)$ denotes a random Gaussian force that satisfies the fluctuation-dissipation theorem, i.e., $\langle\delta F_r(t)\delta F_r(t')\rangle = 2\xi k_B T\delta(t - t')$. We set $k_B T = 1$. We use the velocity-Verlet integrator and the integration time step is 0.002τ, where τ is the reduced time unit, i.e., $\tau \equiv \sqrt{m\sigma^2/k_B T}$.

We use a cubic simulation box of dimension $L = 25\sigma$ with periodic boundary conditions in all directions. Initial configurations are generated by inserting a single polymer chain and matrix particles sequentially at random positions. We grow the polymer by adding monomers without any overlap sequentially. Then, we insert matrix particles without overlaps with preexisting particles until the volume fraction (ϕ) of matrix particles reaches $\phi = \pi\sigma_c^3 N/6L^3$, where N is the total number of matrix particles.

To equilibrate the system, we let all matrix particles diffuse freely such that they are distributed in space with an equilibrium distribution at time $t = 0$. We equilibrate the system until the polymer and matrix particles diffuse at least more than their own size. Then, we select N_m mobile particles and N_o immobile particles (obstacles) randomly; i.e., $N = N_m + N_o$. We fix the obstacles at their own positions during the production simulation runs. $\phi_m = \pi\sigma_c^3 N_m/6L^3$ and $\phi_o = \pi\sigma_c^3 N_o/6L^3$ denote the volume fractions of the mobile and the immobile particles, respectively. The total volume fraction (ϕ) of all matrix particles is, therefore, $\phi = \phi_o + \phi_m$. The ratio of the immobile particles to the total number of matrix particles is $\gamma = N_o/N = \phi_o/\phi$.

To investigate polymer dynamics in crowded environments, we calculate both the mean-square displacement ($\langle[\Delta r(t)]^2\rangle$) and the time correlation function of the end-to-end distance [$C_{\text{ete}}(t)$] of the polymer as follows:

$$\langle[\Delta r(t)]^2\rangle = \langle|\vec{r}(t) - \vec{r}(0)|^2\rangle, \tag{2}$$

$$C_{\text{ete}}(t) = \frac{\langle r_{\text{ete}}(t)r_{\text{ete}}(0)\rangle - \langle r_{\text{ete}}\rangle^2}{\langle r_{\text{ete}}^2\rangle - \langle r_{\text{ete}}\rangle^2}. \tag{3}$$

Here, $\vec{r}(t)$ is the position vector of the center of mass of the chain at time t and $r_{\text{ete}}(t)$ is the end-to-end distance of the chain. $\langle\cdots\rangle$ denotes the ensemble-average. We fit $C_{\text{ete}}(t)$ to an exponential function, i.e., $C_{\text{ete}}(t) \approx \exp(-t/\tau_{\text{ete}})$, and extract the relaxation time τ_{ete}. The polymer conformation is characterized by a probability distribution function [$p(r_{\text{ete}})$] of the end-to-end distance. We also obtain a free-energy profile

$[F(r_{\mathrm{ete}})]$ along the end-to-end distance (a reaction coordinate for the loop formation) by using $F(r_{\mathrm{ete}}) = -k_B T \ln[p(r_{\mathrm{ete}})]$.

The end-to-end distance (r_{ete}) of a polymer chain has been considered as a suitable reaction coordinate for loop formation kinetics [38–40]. Effective diffusion coefficient (D_{ete}) along the reaction coordinate can be estimated by calculating the mean-square displacement ($\langle(\Delta r_{\mathrm{ete}}(t))^2\rangle$) of the polymer end-to-end distance, i.e., $\langle(\Delta r_{\mathrm{ete}}(t))^2\rangle = \langle|r_{\mathrm{ete}}(t) - r_{\mathrm{ete}}(0)|^2\rangle$. $\langle(\Delta r_{\mathrm{ete}})^2\rangle$ is supposed to reach a plateau at sufficiently long times where $\langle(\Delta r_{\mathrm{ete}}(t=\infty))^2\rangle \approx 2\sigma_{\mathrm{ete}}^2 = 2(\langle r_{\mathrm{ete}}^2\rangle - \langle r_{\mathrm{ete}}\rangle^2)$. The diffusion coefficient (D_{ete}) along the reaction coordinate is obtained by using $D_{\mathrm{ete}} = \sigma_{\mathrm{ete}}^2/\tau_{\mathrm{ete}}$.

We decide that a loop forms when r_{ete} is smaller than a contact distance (r_{loop}). We set the value of $r_{\mathrm{loop}} = 1.8\sigma$ to the value of r_{ete} at a local minimum in $p(r_{\mathrm{ete}})$ [Fig. 2(a)]. We calculate the mean-first passage times (τ_{loop} and τ_{unloop}) for looping and unlooping processes, respectively. The survival probability [$S(t)$] of looping (unlooping) reaction is defined by a probability for a looped (unlooped) polymer to remain in the same state after time t. We fit the simulation results for $S(t)$ to a stretched exponential function of $S(t) = \exp[-(t/\tau)^\beta]$. β is a measure of how heterogeneous the reaction kinetics is.

III. RESULTS AND DISCUSSION

A. The pore percolation transition of the system

The diffusion of macromolecules in porous media depends significantly on the volume fraction (ϕ_o) of immobile matrix particles [30,41,42]. When ϕ_o is larger than its critical value (ϕ_c) at the pore percolation transition, no percolating free volume exists such that the macromolecules do not diffuse at long timescales. Then, the mean-square displacement ($\langle[\Delta r(t)]^2\rangle$) is not linear with time t at long times but rather reaches a plateau. Only when $\phi_o < \phi_c$ and a macromolecule is placed within a percolating free volume, the macromolecule undergoes the Brownian diffusion at long timescales and $\langle[\Delta r(t)]^2\rangle \sim t^1$. At the percolation threshold of $\phi_o = \phi_c$, the free volume is fractal at all length scales and the macromolecules should undergo the subdiffusion at all spatiotemporal scales.

Figure 1(a) depicts the mean-square displacement ($\langle[\Delta r(t)]^2\rangle$) of the center of mass of the polymer chain in our study for small matrix particles ($\sigma_c = 1\sigma$) of $\phi = 0.05$ and 0.1. Note that the fraction (γ) of immobile particles varies from 0 to 0.8. For a given value of the total volume fraction (ϕ) of matrix particles, the diffusion slows down as γ increases. When $\phi = 0.1$ and $\gamma = 0.8$, the polymer diffusion becomes anomalous, i.e., $\langle[\Delta r(t)]^2\rangle \sim t^{0.7}$ at several orders of magnitude of time. Such anomalous subdiffusion is also observed for large matrix particles at sufficiently large values of γ and ϕ.

The values of ϕ_c for the pore percolation transition depends on the sizes of both matrix particles and polymers (macromolecules). It is not a trivial task to determine the exact value of ϕ_c for polymers in random porous media, especially when intermolecular interactions are a continuous function instead of a hard-sphere interaction (where an exact estimate of the free volume is allowed). One also has to take the finite-size
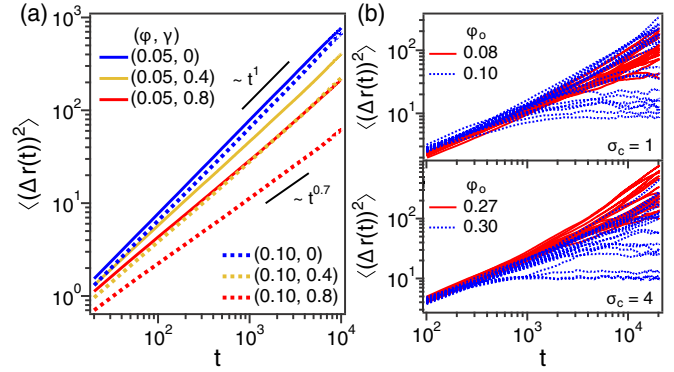
FIG. 1. (a) The mean-square displacement $\langle[\Delta r(t)]^2\rangle$ of the center of mass of the polymer chain for different values of ϕ and γ of matrix particles of $\sigma_c = 1$. (b) $\langle[\Delta r(t)]^2\rangle$'s of independent trajectories in 20 different matrix configurations for different values of ϕ_o with $\gamma = 1$ (the upper panel for $\sigma_c = 1$ and the lower panel for $\sigma_c = 4$).

scaling behavior into account to pinpoint the value of ϕ_c, which is also beyond the scope of the current study. Instead, we plan to estimate the approximate range of ϕ_c by observing $\langle[\Delta r(t)]^2\rangle$ for each matrix configuration.

Figure 1(b) shows $\langle[\Delta r(t)]^2\rangle$'s of 20 independent trajectories in 20 different matrix configurations, which start from different initial configurations of small (upper panel) and large (lower panel) matrix particles. Note that while mobile matrix particles diffuse freely, immobile matrix particles are fixed at initial positions during the simulations such that the matrix configuration of one trajectory is different from others. Therefore, the transport properties of a chain in 20 matrix configurations would differ from one another, especially near the percolation transition.

Above a certain volume fraction of immobile particles near the percolation threshold, the *confined diffusion* would appear such that $\langle[\Delta r(t)]^2\rangle$ reaches a plateau at long times. As shown in Fig. 1(b), the volume fraction at which the confined diffusion begins to appear depends on the size of matrix particles ($\sigma_c = 1$ and 4). In case of $\sigma_c = 1$ (upper panel), all $\langle[\Delta r(t)]^2\rangle$'s of 20 trajectories show a diffusive behavior at for $\phi_o \leqslant 0.08$ but the confined diffusion begins to appear for $\phi_o = 0.1$. This indicates that ϕ_c lies between $\phi_o = 0.08$ and 0.1. Similarly, ϕ_c lies between $\phi_o = 0.27$ and 0.3 for large matrix particles (lower panel). We also confirmed that the volume fraction where the confined diffusion appears depends only on ϕ_o regardless of γ and ϕ investigated in our study.

B. The structure and dynamics of the polymer chain

The kinetics of a chemical reaction is determined mostly by (1) the free-energy barrier ($\Delta F^\ddagger$) and (2) the effective diffusion coefficient (D_{ete}) along the reaction coordinate, i.e., the end-to-end distance (r_{ete}). D_{ete} relates to how fast the reactant samples the phase space and crosses the free-energy barrier. Therefore, D_{ete} determines the pre-exponential factor of the Arrhenius equation. In this section, we estimate D_{ete} and the free-energy profile [$\Delta F(r_{\mathrm{ete}})$] as a function of r_{ete} by calculating the distribution function [$p(r_{\mathrm{ete}})$] of r_{ete} and using $\Delta F(r_{\mathrm{ete}}) = -k_B T \ln[p(r_{\mathrm{ete}})]$.
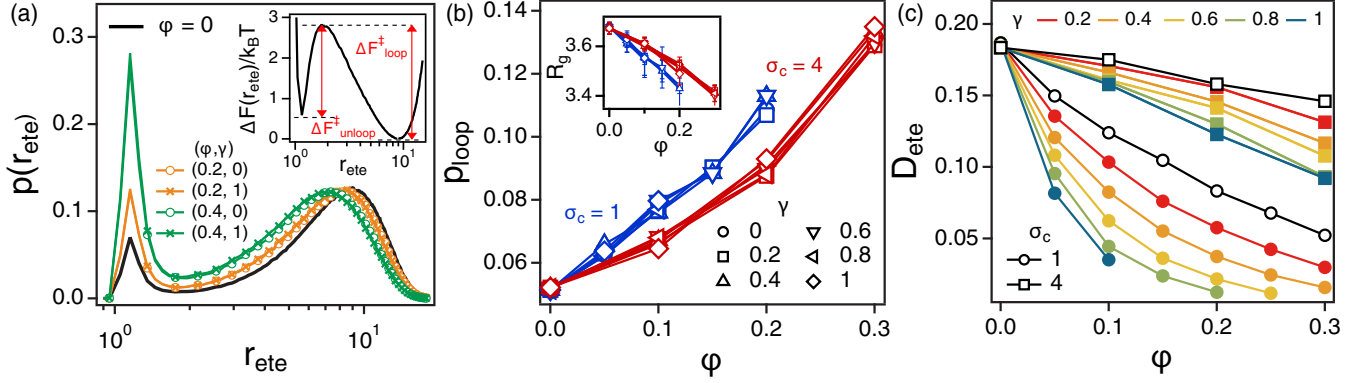
FIG. 2. (a) Probability distribution functions [$p(r_{ete})$] of the end-to-end distance of a polymer chain at different values of ϕ and γ. A black solid line indicates $p(r_{ete})$ of a polymer chain in a solution without matrix particles. (Inset) The free-energy profiles ($\Delta F(r_{ete})/k_B T = -\ln[p(r_{ete})]$) as a function of r_{ete}. (b) The probability (p_{loop}) of the polymer chain being looped as a function of ϕ for small and large matrix particles. (Inset) The radius of gyration (R_g) of the polymer. (c) The diffusion coefficient (D_{ete}) of the end-to-end distance (r_{ete}) as a function of ϕ for different values of γ and σ_c. Black symbols represent D_{ete} with $\gamma = 0$ at a given ϕ.

Figure 2(a) depicts $p(r_{ete})$ for the systems of large matrix particles. The attractive interaction between two ends of the polymer chain results in the bimodal distribution of r_{ete} and consequently the double-well free-energy profile [$\Delta F(r_{ete})$]. We divide the polymer conformation into a looped and an un-looped states by employing a criterion of $r_{loop} \approx 1.8\sigma$, which is the location of the local minimum of $p(r_{ete})$ [Fig. 2(a)]. Without any matrix particles [a black solid line in Fig. 2(a)], an unlooped state is more stable than a looped state due to the large conformational entropy for unlooped states. As we introduce matrix particles (with an increase in ϕ), the proba-bility of the polymer being in the looped state becomes higher. For the highest value of $\phi = 0.4$ in this study, the looped state becomes more stable by about $1k_B T$ than the unlooped state as in the inset of Fig. 2(a). The radius of gyration (R_g) of the polymer [inset in Fig. 2(b)] is also decreased as the system gets more crowded with more matrix particles. It is well-known from previous experiments and simulations that the crowding effects lead to a smaller size of macromolecules due to the excluded volume interactions [5,43–45].

Interestingly, both $p(r_{ete})$ and $\Delta F(r_{ete})$ are not subject to the fraction (γ) of immobile crowders [Fig. 2(a)]. For a given value of ϕ, $p(r_{ete})$'s are all identical within statistical error bars regardless of γ. This indicates that the free-energy profile and free-energy barrier for the reaction are determined not by the mobility of matrix particles but by their density. We also calculate the probability (p_{loop}) that a polymer chain forms a loop by using $p_{loop} = \int_0^{r_{loop}} p(r_{ete}) dr_{ete}$. As depicted in Fig. 2(b), for a given size (σ_c) of matrix particles, p_{loop}'s overlap as a function of ϕ for different values of γ.

Figure 2(b) also shows that for a given volume fraction (ϕ) of matrix particles, a polymer chain in media of smaller particles is more likely to form a loop than in media of larger particles. This leads to a smaller radius of gyration (R_g) of the polymer chain [the inset of Fig. 2(b)] and a deeper free-energy minimum at the looped state in the media of smaller matrix particles. Such a deep free-energy minimum arises because small matrix particles tend to create large excluded volume more easily than large matrix particles, which makes unlooped (extended) conformations less favorable.

While both $p(r_{ete})$ and $\Delta F(r_{ete})$ are not subject to the fraction (γ), the rate of conformational change is sensitive significantly to γ. Figure 2(c) depicts the diffusion coefficient (D_{ete}) of the end-to-end distance as a function of ϕ. Black lines indicate the values of D_{ete} for $\gamma = 0$ when all matrix particles are mobile. For $\gamma = 0$, D_{ete} decreases gradually with an increase in ϕ. For large matrix particles of $\sigma_c = 4\sigma$, D_{ete} decreases by about 21% as ϕ increases from 0 to 0.3. However, for small matrix particles of $\sigma_c = 1\sigma$, D_{ete} decreases by about 65%.

As γ increases and more matrix particles become immo-bile, D_{ete} decreases quickly even for large matrix particles. In case of small matrix particles, the decrease of D_{ete} due to immobile particles is more prominent. When ϕ_o becomes sufficiently high, the polymer chain even fails to undergo conformational relaxation such that $C_{ete}(t)$ hardly decays with time and we cannot estimate the value of D_{ete}. We find that the conformational relaxation still occurs slightly above the percolation threshold with $\phi_o > \phi_c$ where the translational diffusion of the center of mass of the chain vanishes. When ϕ_o exceeds ϕ_c far enough, the conformational relaxation does not occur such that τ_{ete} goes to infinity, $D_{ete} = 0$. For example, in Fig. 2(c), in the case of $\phi_o \geqslant 0.16 > \phi_c \approx 0.1$ for small crowders, we cannot estimate τ_{ete} and consequently D_{ete}.

C. The kinetics of the looping and the unlooping of the polymer chain

In this subsection, we investigate the kinetics of both looping and unlooping of a polymer chain in crowded environ-ments. In general, the reaction is expected to slow down when either the free-energy barrier ($\Delta F^{\ddagger}$) increases or the effective diffusion coefficient (D_{ete}) decreases.

First, we investigate the kinetics in crowded solutions where all matrix particles are free to diffuse ($\gamma = 0$). In Fig. 3(a), the looping time (τ_{loop}) and the unlooping time (τ_{unloop}) are plotted as a function of $\phi = \phi_m$ for two different sizes of matrix particles. In case of looping (upper panel), τ_{loop} shows a different trend depending on the sizes of crow-ders: τ_{loop} increases with an increase in ϕ for small matrix
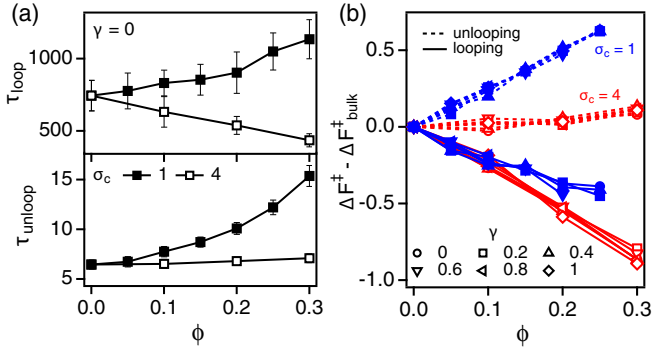
FIG. 3. (a) The looping time (τ_{loop}) and unlooping time (τ_{unloop}) as functions of ϕ when all matrix particles are mobile ($\gamma = 0$). (b) The free-energy barrier difference ($\Delta F^{\ddagger} - \Delta F^{\ddagger}_{bulk}$) between polymers in porous media ($\phi \neq 0$) and bulk solutions ($\phi = 0$).

particles while τ_{loop} decreases with ϕ for large matrix particles. However, in case of unlooping (lower panel), τ_{unloop} increases with an increase in ϕ regardless of the matrix particle size. However, the increase in τ_{unloop} is not significant for larger matrix particles.

Figure 3(b) shows how the free-energy barrier of looping ($\Delta F^{\ddagger}_{loop}$) and unlooping ($\Delta F^{\ddagger}_{unloop}$) change with ϕ. The definitions of $\Delta F^{\ddagger}_{loop}$ and $\Delta F^{\ddagger}_{loop}$ are described in the inset of Fig. 2(a). $\Delta F^{\ddagger}_{bulk}$ denotes the value of either $\Delta F^{\ddagger}_{loop}$ or $\Delta F^{\ddagger}_{unloop}$ when there is no matrix particle ($\phi = 0$), which are $2.8 k_B T$ for looping and $2.2 k_B T$ for unlooping. In case of looping, the free-energy barrier $\Delta F^{\ddagger}_{loop}$ decreases as more matrix particles are introduced, for which $\Delta F^{\ddagger}_{loop} - \Delta F^{\ddagger}_{bulk} \leqslant 0$. This indicates that if one considers only the free-energy barrier, the reaction would become faster and τ_{loop} would decrease as ϕ is increased. At the same time, if one considers only D_{ete} (, which decreases with an increase in ϕ), τ_{loop} is expected to increase. Therefore, τ_{loop} is determined by the competing effects of $\Delta F^{\ddagger}_{loop}$ and D_{ete}. For large matrix particles, the decrease in D_{ete} is marginal such that a decrease in $\Delta F^{\ddagger}_{loop}$ overwhelms a weak slowdown in D_{ete}, and hence τ_{loop} decreases with ϕ. However, for small matrix particles, a substantial slowdown in effective diffusion (a decrease in D_{ete}) overwhelms a relatively weak decrease of ΔF_{loop}, which leads to an increase in τ_{loop}.

In case of unlooping, $\Delta F^{\ddagger}_{unloop}$ increases with ϕ because the looped state becomes more stable. As shown in Fig. 3(b), therefore, $\Delta F^{\ddagger}_{unloop} - \Delta F^{\ddagger}_{bulk}$ increases with ϕ. In case of small matrix particles ($\sigma_c = 1\sigma$), the increase in $\Delta F^{\ddagger}_{unloop}$ is significant because the free volume of the system may be excluded more effectively with small matrix particles. Both the decrease in D_{ete} and the increase in $\Delta F^{\ddagger}_{unloop}$ (with an increase in ϕ) lead to the slower kinetics of unlooping, for which τ_{unloop} increases with ϕ regardless of the matrix particle size. The increase in τ_{unloop} for large matrix particles is relatively moderate because changes in both D_{ete} and $\Delta F^{\ddagger}_{unloop}$ are moderate compared to those of small matrix particles. Our results for $\gamma = 0$ with only mobile matrix particles are consistent with previous works by Shin et al. [17,46].

Figure 4 depicts how the heterogeneous dynamics (that arises due to the immobile particles) would affect the kinetics of looping and unlooping. Because $\Delta F^{\ddagger}_{loop}$ and $\Delta F^{\ddagger}_{unloop}$ do not change with γ at a given ϕ, only the effects of γ on D_{ete} would affect τ_{loop} and τ_{unloop}. Figures 4(a) and 4(b) depict τ_{loop} of different values of γ in media of small and large matrix particles. For small matrix particles [Fig. 4(a)], τ_{loop} increases with ϕ much more sharply as we increase γ because D_{ete} is decreased tremendously with γ. For large crowders [Fig. 4(b)], τ_{loop} gradually decreases when $\gamma = 0.2$. But, τ_{loop} begins to increase as γ increases at a given ϕ. And it shows even a nonmonotonic behavior when $\gamma \geqslant 0.4$, because a slowdown in D_{ete} is so prominent with $\gamma \geqslant 0.4$.

However, there is no significant change in τ_{unloop} with γ at a given ϕ as shown in Fig. 4(c). This implies that the unlooping of the polymer is marginally affected by D_{ete}. This is because unlooping of the polymer occurs within a short length scale where $r_{ete} \leqslant 1.8\sigma$, while D_{ete} is involved with the longest relaxation modes of the polymer.

D. Heterogeneous loop formation kinetics above the percolation threshold

As ϕ_o nears ϕ_c, the pore structure becomes quite heterogeneous as in previous studies [30,47]. For $\phi_o < \phi_c$, there exists a percolating pore network. At the same time, there are large but isolated and non-percolating pores that are tortuous around the percolation threshold. The percolation, size and tortuosity of pores affect the translational diffusion
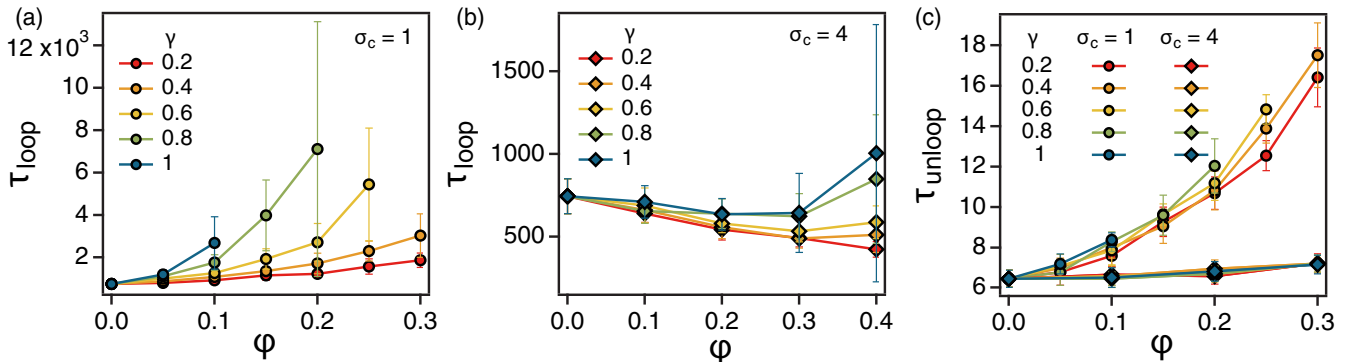
FIG. 4. The looping time (τ_{loop}) as a function of ϕ in media of (a) small and (b) large matrix particles. Different colors indicate different values of γ. (c) The unlooping time (τ_{unloop}) as a function of ϕ for different values of σ_c and γ.

of molecules in porous media all together. In the previous subsection, we find that $\phi_c \approx 0.1$ and 0.3 for small and large matrix particles, respectively. In this subsection, we investigate how the kinetics of looping and unlooping becomes heterogeneous near the percolation threshold in such heterogeneous environments.

To characterize the heterogeneity in kinetics, we calculate the relative deviation ($\delta_{\rm rel}$) defined as $\delta_{\rm rel} \equiv \delta_{\rm (un)loop}/\tau_{\rm (un)loop}$, where $\delta_{\rm (un)loop}$ is the standard deviation of (un)looping times of 20 independent trajectories. We also investigate how the survival probabilities [$S(t)$] of looping and unlooping reactions decay with time t to characterize the heterogeneity in kinetics. We fit the simulation results for $S(t)$ to the stretched exponential function of $S(t) = \exp[-(t/\tau)^\beta]$ and obtain the value of β. In case reactions occur homogeneously with a single reaction rate constant, $\beta = 1$. If the reaction kinetics becomes dispersed and heterogeneous with different reaction rate constants, $S(t)$ becomes stretched with $\beta < 1$. Such stretched exponential decay has been reported for various systems where different relaxation times existed [48–51]. The deviation of β from unity, therefore, reflects how much the reaction kinetics is dispersed.

Figure 5 depicts $\delta_{\rm rel}$ and β of looping and unlooping kinetics as a function of ϕ_o. Note that we plot all data points with different values of ϕ (and ϕ_m). We check all data points and find that $\delta_{\rm rel}$ and β depend hardly on ϕ but mostly on ϕ_o. We mark the region where ϕ_c is likely to be located with blue and red bands for small and large matrix particles in the Fig. 5. In case of looping (filled symbols), $\delta_{\rm rel}$ is around 0.15 when $\phi_o \leqslant \phi_c$. Interestingly, however, $\delta_{\rm rel}$ increases sharply as ϕ_o approaches ϕ_c in media of both small and large matrix particles. This implies that the reaction rate of loop formation becomes heterogeneous significantly near the percolation threshold. Similarly, β of looping kinetics decreases from unity to 0.6 as ϕ_o approaches ϕ_c.

However, $\delta_{\rm rel}$ and β of unlooping kinetics do not change much with ϕ_o even near the percolation threshold. As shown in Fig. 3(c), the unlooping kinetics is hardly correlated with γ. Unlooping of a polymer chain occurs much faster than looping and is not affected by $D_{\rm ete}$ much [Fig. 4(c)]. This implies that while unlooping, the polymer would have less chance to collide with obstacles and experience the spatial heterogeneity. This would make the unlooping kinetics of the polymer chain remain homogeneous even when the dynamics and structure of matrix particles become heterogeneous.

Our simulation results for $\delta_{\rm rel}$ and β indicate that as ϕ_o reaches ϕ_c and the pore structure becomes heterogeneous, the kinetics of looping becomes dispersed and heterogeneous, too. To investigate how the loop formation rate correlates with local heterogeneous environments, we perform following analyses. For a given set of (ϕ, γ), we let $\tau_{{\rm loop},i}$ denote the looping time for the polymer chain in the ith configuration among 20 different matrix configurations. $\tau_{\rm loop}$ and δ are the average and the standard deviation of 20 values of $\tau_{{\rm loop},i}$. Then, we divide 20 configurations into three groups depending on the value of $\tau_{{\rm loop},i}$: *slow* looping, *moderate* looping, and *fast* looping as follows: \$1) slow looping: $\tau_{{\rm loop},i} > \tau_{\rm loop} + \delta$, \$2) moderate looping: $|\tau_{{\rm loop},i} - \tau_{\rm loop}| < \delta$, \$3) fast looping: $\tau_{{\rm loop},i} < \tau_{\rm loop} + \delta$.
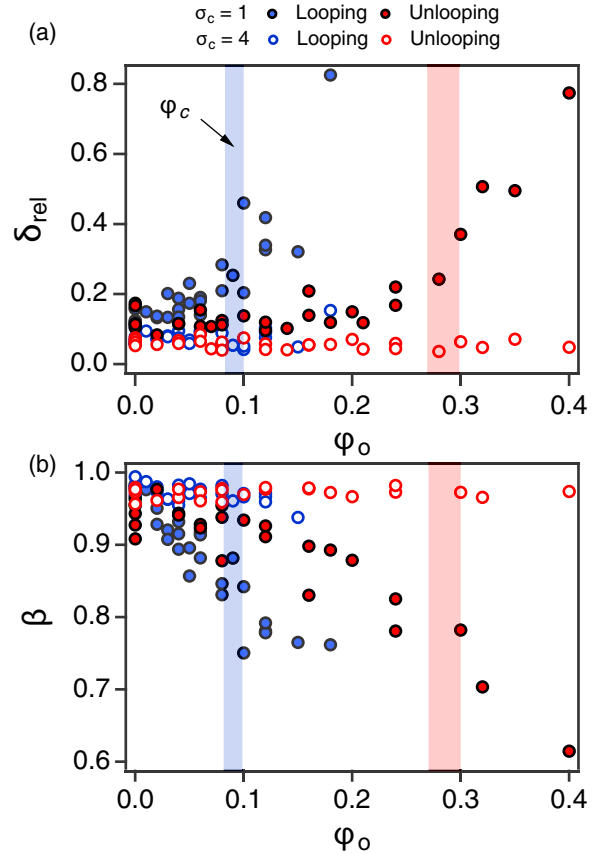
FIG. 5. (a) Relative deviation ($\delta_{\rm rel}$) for looping and unlooping times as a function of ϕ_o in the media of large and small matrix particles. (b) β of the stretched exponential function as a function of ϕ_o in media of large and small matrix particles. In both (a) and (b), blue- and red-shaded bands represent the ranges where the percolation threshold concentrations (ϕ_c's) are located for small and large matrix particles, respectively.

We find that there is a strong correlation between a local pore geometry and looping time: A confined polymer forms a loop faster. Figure 6(a) shows $\langle (\Delta r(t))^2 \rangle$ of the polymer center of mass for 20 individual trajectories in porous media of $\sigma_c = 4\sigma$, $\phi_o = 0.4$, and $\phi_m = 0$. Different colors represent different groups defined above: Slow (red), moderate (yellow), and fast (blue) looping groups. Because the volume fraction of immobile crowders exceeds the percolation threshold ($\phi_c \approx 0.3$) in this figure, there are different sizes of nonpercolating local pores: Some of them are large enough for the polymer to diffuse at small length scales but cannot diffuse at long timescales and others are so small that a polymer hardly move and $\langle [\Delta r(t)]^2 \rangle$ reaches a plateau quickly. As shown in Figure 6(a), there is a clear correlation between the looping time and the local structure: (i) Polymers in the slow looping group tend to diffuse well translationally (at short timescales) and (ii) polymers in the fast looping group are confined and hardly diffuse such that $\langle [\Delta r(t)]^2 \rangle$ reaches a plateau even at short times.

We also investigate how the looping time ($\tau_{{\rm loop},i}$) would relate with the distribution [$p(r_{\rm ete})$] of $r_{\rm ete}$ and the time correlation function [$C_{\rm ete}(t)$] of $r_{\rm ete}$. As shown in Figs. 6(b) and
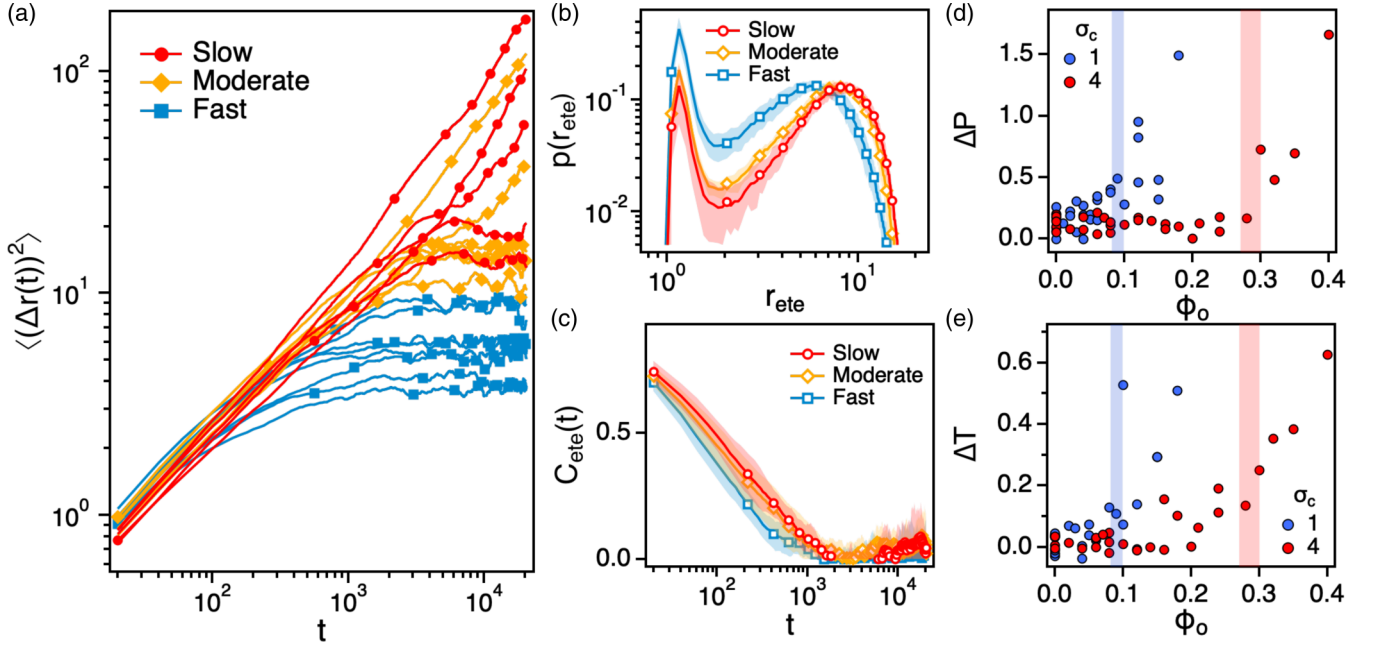
FIG. 6. (a) $\langle(\Delta r(t))^2\rangle$'s of 20 independent trajectories in different matrix configurations of large matrix particles of $\phi_o = 0.4$ ($\gamma = 1$). (b) $p(r_{ete})$ for each group with different looping rate. (c) $C_{ete}(t)$ for each group with different looping rate. In both (b) and (c), the statistical errors of one standard deviation are indicated with shaded area. (d) $\Delta P \equiv (p_s - p_f)/p_m$ as a function of ϕ_o. (e) $\Delta T \equiv (\tau_s^{-1} - \tau_f^{-1})/\tau_m^{-1}$ as a function of ϕ_o. The blue and red shaded bands represent the ranges where the percolation threshold concentrations (ϕ_c's) are located for small and large matrix particles, respectively.

6(c), the looping time of each configuration shows a clear correlation with both $p(r_{ete})$ and $C_{ete}(t)$. Polymer chains in the slow looping group are more likely to be extended such that the slow looping polymers have higher $p(r_{ete})$ at a large r_{ete} than the moderate and fast looping polymers. And $C_{ete}(t)$ of the slow looping group decays much slower than those of fast and moderate looping groups. This suggests that a polymer chain in relatively large pores are likely to diffuse faster but is extended such that the conformational relaxation slows down, for which the loop formation process becomes slow.

The heterogeneous kinetics and the difference between different looping groups become prominent near the percolation transition. To investigate the differences in polymer conformation and conformational relaxation time among three groups, we estimate both the probability of a polymer chain forming a loop and the relaxation time of $C_{ete}(t)$ for each group. p_s, p_m, and p_f stand for the probabilities of a polymer chain in slow, moderate, and fast looping groups forming a loop, respectively. For example, p_s is calculated by using $p(r_{ete})$ for the slow group and $p_s = \int_0^{r_{loop}} p(r_{ete}) dr_{ete}$. Similarly, τ_s, τ_m, and τ_f denote the relaxation times obtained from $C_{ete}(t)$ in slow, moderate, and fast looping groups, respectively.

Figures 6(d) and 6(e) depict $\Delta P \equiv (p_f - p_s)/p_m$ and $\Delta T \equiv (\tau_f^{-1} - \tau_s^{-1})/\tau_m^{-1}$, respectively. If there were to be no correlation, $\Delta P \approx 0$ and $\Delta T \approx 0$. As the polymer conformation becomes heterogeneous and strongly correlated with the loop formation, however, ΔP and ΔT should increase. As shown in Figs. 6(d) and 6(e), $\Delta P \approx 0$ and $\Delta T \approx 0$ when $\phi_o < \phi_c$, implying that below the percolation transition, the loop formation kinetics is hardly correlated with the polymer conformation and its relaxation time. However, as ϕ_o approaches

ϕ_c, both ΔP and ΔT increase sharply, suggesting that the heterogeneous loop formation kinetics would result from the spatial heterogeneity of the medium due to the presence of immobile obstacles surrounding the polymer.

IV. CONCLUSION

In this study, we investigate the kinetics of looping and unlooping of a single polymer chain in crowded and disordered environments. We tune the degree of dynamic heterogeneity of matrix particles by changing the fraction (γ) of the number of immobile particles: $\gamma = 0$ corresponds to when all matrix particles diffuse while all matrix particles are immobile for $\gamma = 1$. We investigate the translational diffusion of the center of mass of the polymer chain to characterize the pore percolation transition threshold (ϕ_c).

As the volume fraction (ϕ) of total matrix particles increases, the size of the polymer becomes smaller and the free-energy barrier ($\Delta F^{\ddagger}$) for looping (unlooping) increases (decreases). Meanwhile, the diffusion (D_{ete}) of the end-to-end distance becomes slower as we increase ϕ. The rates of looping and unlooping are determined by a balance between $\Delta F^{\ddagger}$ and D_{ete}, for which the kinetics of looping and unlooping shows complicated behaviors depending on the matrix particle size.

As the volume fraction (ϕ_o) of immobile particles reaches the pore percolation threshold concentration (ϕ_c), the pore structures become heterogeneous such that the kinetics of looping becomes also dispersed and heterogeneous significantly. However, the unlooping is not influenced much by the value of γ. We investigate the correlation between the

local heterogeneous structure and the looping kinetics, and find that a polymer chain in a relatively large pore is more likely to be extended and perform a slower conformational relaxation. This leads to a slow looping kinetics for the polymer chain. Such a correlation between the local structure and the looping kinetics becomes significant near and beyond the pore percolation transition.

[1] H.-X. Zhou, G. Rivas, and A. P. Minton, Annu. Rev. Biophys. **37**, 375 (2008).

[2] S. B. Zimmerman and S. O. Trach, J. Mol. Biol. **222**, 599 (1991).

[3] J. A. Dix and A. S. Verkman, Annu. Rev. Biophys. **37**, 247 (2008).

[4] D. Homouz, M. Perham, A. Samiotakis, M. S. Cheung, and P. Wittung-Stafshede, Proc. Natl. Acad. Sci. USA **105**, 11754 (2008).

[5] B. van den Berg, R. Wain, C. M. Dobson, and R. J. Ellis, EMBO J. **19**, 3870 (2000).

[6] B. van den Berg, R. J. Ellis, and C. M. Dobson, EMBO J. **18**, 6927 (1999).

[7] A. Christiansen and P. Wittung-Stafshede, FEBS Lett. **588**, 811 (2014).

[8] H.-X. Zhou, FEBS Lett. **587**, 1053 (2013).

[9] H.-X. Zhou, J. Mol. Recognit. **17**, 368 (2004).

[10] A. Kudlay, M. S. Cheung, and D. Thirumalai, J. Phys. Chem. B **116**, 8513 (2012).

[11] A. Vazquez and Z. N. Oltvai, Sci. Rep. **6**, 31007 (2016).

[12] S. Smith, C. Cianci, and R. Grima, J. R. Soc., Interface **14**, 20170047 (2017).

[13] F. Höfling and T. Franosch, Rep. Prog. Phys. **76**, 046602 (2013).

[14] J. M. Rohwer, P. W. Postma, B. N. Kholodenko, and H. V. Westerhoff, Proc. Natl. Acad. Sci. USA **95**, 10547 (1998).

[15] Y. Bian, X. Cao, P. Li, and N. Zhao, Soft Matter **14**, 8060 (2018).

[16] S. Mukherjee, M. M. Waegele, P. Chowdhury, L. Guo, and F. Gai, J. Mol. Biol. **393**, 227 (2009).

[17] J. Shin, A. G. Cherstvy, and R. Metzler, Soft Matter **11**, 472 (2014).

[18] B. J. Sung, R. Chang, and A. Yethiraj, J. Chem. Phys. **130**, 124908 (2009).

[19] B. J. Sung and A. Yethiraj, J. Chem. Phys. **126**, 034704 (2007).

[20] B. J. Sung and A. Yethiraj, Phys. Rev. Lett. **96**, 228103 (2006).

[21] H. W. Cho, A. Yethiraj, and B. J. Sung, Sci. Rep. **9**, 251 (2019).

[22] S. F. Edwards and M. Muthukumar, J. Chem. Phys. **89**, 2435 (1988).

[23] J. D. Honeycutt and D. Thirumalai, J. Chem. Phys. **90**, 4542 (1989).

[24] S. Shanbhag, J. Polym. Sci. Pol. Phys. **53**, 1611 (2015).

[25] A. Milchev, J. Phys.: Condens. Matter **23**, 103101 (2011).

[26] V. Blavatska and W. Janke, J. Chem. Phys. **133**, 184903 (2010).

[27] M. Muthukumar and A. Baumgaertner, Macromolecules **22**, 1941 (1989).

[28] A. Baumgärtner and M. Muthukumar, Adv. Chem. Phys. **XCIV**, 625 (1996).

[29] Z. E. Dell and M. Muthukumar, J. Chem. Phys. **149**, 174902 (2018).

[30] H. Jeon, H. W. Cho, J. Kim, and B. J. Sung, Phys. Rev. E **90**, 042105 (2014).

[31] M. P. Lettinga, C. M. van Kats, and A. P. Philipse, Langmuir **16**, 6166 (2000).

[32] P. Massignan, C. Manzo, J. A. Torreno-Pina, M. F. García-Parajo, M. Lewenstein, and G. J. Lapeyre, Phys. Rev. Lett. **112**, 150603 (2014).

[33] K. Kim, K. Miyazaki, and S. Saito, Europhys. Lett. **88**, 36002 (2009).

[34] R. Afra and B. A. Todd, J. Chem. Phys. **138**, 174908 (2013).

[35] S. Jun, J. Bechhoefer, and B. Y. Ha, Europhys. Lett. **64**, 420 (2003).

[36] R. B. Best and G. Hummer, Phys. Rev. Lett. **96**, 228104 (2006).

[37] S. J. Hagen, Curr. Protein Pept. Sci. **11**, 385 (2010).

[38] A. Szabo, K. Schulten, and Z. Schulten, J. Chem. Phys. **72**, 4350 (1980).

[39] G. Wilemski and M. Fixman, J. Chem. Phys. **60**, 866 (1974).

[40] N. M. Toan, G. Morrison, C. Hyeon, and D. Thirumalai, J. Phys. Chem. B **112**, 6094 (2008).

[41] B. J. Sung and A. Yethiraj, J. Phys. Chem. B **112**, 143 (2008).

[42] H. W. Cho, G. Kwon, B. J. Sung, and A. Yethiraj, Phys. Rev. Lett. **109**, 155901 (2012).

[43] J. Adén and P. Wittung-Stafshede, Biochemistry **53**, 2271 (2014).

[44] H.-X. Zhou, Arch. Biochem. Biophys. **469**, 76 (2008).

[45] X.-W. Huang, Y. Peng, and J.-H. Huang, Colloid Polym. Sci. **296**, 689 (2018).

[46] J. Shin, A. G. Cherstvy, and R. Metzler, ACS Macro Lett. **4**, 202 (2015).

[47] B. J. Sung and A. Yethiraj, J. Chem. Phys. **128**, 054702 (2008).

[48] J. Kakalios, R. A. Street, and W. B. Jackson, Phys. Rev. Lett. **59**, 1037 (1987).

[49] J. C. Phillips, Rep. Prog. Phys. **59**, 1133 (1996).

[50] W. Min and X. S. Xie, Phys. Rev. E **73**, 010902(R) (2006).

[51] D. C. Johnston, Phys. Rev. B **74**, 184430 (2006).